THE JOURNAL OF PHYSICAL CHEMISTRY C

Article

pubs.acs.org/JPCC

Pressure-Induced Phase Transition in N–H···O Hydrogen-Bonded Molecular Crystal Biurea: Combined Raman Scattering and X-ray Diffraction Study

Tingting Yan,[†] Kai Wang,*[,†] Xiao Tan,[†] Ke Yang,[‡] Bingbing Liu,[†] and Bo Zou*[,†]

[†]State Key Laboratory of Superhard Materials, Jilin University, Changchun 130012 China

[‡]Shanghai Synchrotron Radiation Facilities, Shanghai Institute of Applied Physics, Chinese Academy of Sciences, Shanghai 201204, China

Supporting Information

ABSTRACT: The response of biurea to high pressures is investigated by *in situ* Raman spectroscopy and angle-dispersive X-ray diffraction (ADXRD) in a diamond anvil cell up to ~5 GPa. Raman scattering measurements indicate a phase transition occurring over the pressure range of 0.6–1.5 GPa. Phase transition is confirmed by changes in the ADXRD spectra with symmetry transformation from $C2/c$ to a possible space group $P2/n$. Upon total release of pressure, the diffraction spectrum returns to its initial state, which implies that the transition observed is reversible. We discuss variations in the Raman spectra, including splitting of modes, appearance of new modes, and abrupt changes in the slope of the frequency shift curves at several pressures. We propose that the phase transition observed in this study is attributed to rearrangement of the hydrogen-bonded networks.

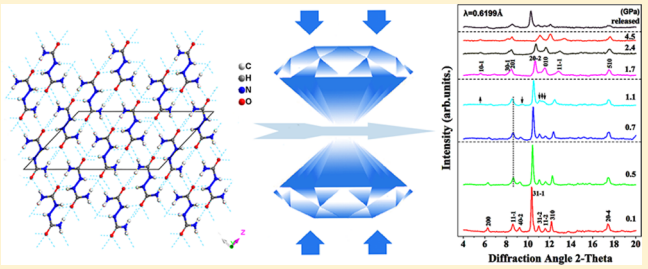

INTRODUCTION

As a pervasive noncovalent interaction, hydrogen bonding is consistently the subject of extensive research, because of its importance in determining the structural stability, function, and dynamics of chemical systems.[1−6] Especially, high pressure can serve as a very efficient tool for studying hydrogen-bonded systems. Rearrangement in hydrogen-bonded networks can easily be promoted by compression.[7,8] Moreover, pressure can break and form hydrogen bonds[9,10] as well as induce symmetrization and proton disorder.[11−16] In addition, compression of materials can facilitate close packing, which alters the balance between hydrogen bonding and van der Waals interactions, resulting in new molecular reorientations and rearrangements.[17−20] The physicochemical properties of solid materials are strongly related to their structures. Hence, high-pressure investigations of hydrogen-bonded molecular crystals are essential to acquire further knowledge on structure–property relationships. Such investigations are also of fundamental and practical significance for physics, chemistry, and materials science.

Over the past few decades, considerable effort has been devoted to studying hydrogen-bonded crystals under high pressures. Rich phenomena have been observed and analyzed. The complex phase diagram in ice continues to attract scientists' attention and is still being investigated; of significant interest is partially ionic characteristic at extremely high pressure (2 TPa) and high temperature (2000 K).[21−26] Natural amino acids such as glycine,[27] serine,[28] and alanine,[29] which are linked by hydrogen bonds between the ammonium and carboxylate groups, also show polymorphism at elevated pressures. As a typical supramolecular architecture, guanidinium nitrate undergoes a phase transition at 1 GPa; this transition is associated with the collapse of the 2-D layered structure into a 3-D stereostructure.[30] Urea, a textbook example of hydrogen-bonded molecular crystals, has been investigated systematically under high pressures.[31−39] Three high-pressure phases of urea crystals have been observed during compression of single-crystal and polycrystalline samples at pressures of up to 12 GPa. Observations of crystals grown in a diamond anvil cell show that the ambient phase I undergoes phase transition at 0.48 GPa, yielding phase III. Phase II, which is solved by neutron-scattering studies of polycrystalline deuterated urea, typically refers to the inclusion compound phase of urea. Further increases in pressure to 2.8 GPa result in another transition to phase IV. Compared with the other polymorphs, the orientations of urea molecules appear significantly altered during these phase transitions. The high-pressure behavior of thiourea, the molecular formula and structure of which are similar to those of urea except that the O atom in urea is replaced by S, also exhibits various structural changes.[40−42] Four phase transitions take place during high-pressure Raman scattering measurements of thiourea. These results suggest that

Received: April 18, 2014
Revised: June 22, 2014
Published: June 26, 2014

   dx.doi.org/10.1021/jp503803n | *J. Phys. Chem. C* 2014, 118, 15162–15168

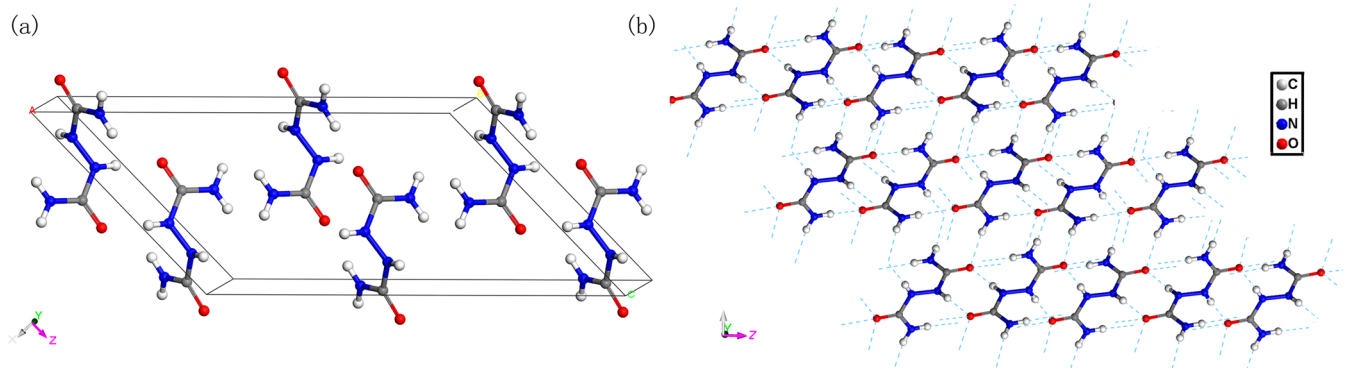

Figure 1. Crystal structure of biurea under ambient conditions: (a) unit cell; (b) hydrogen-bonded networks. The hydrogen bonds are denoted by dashed lines.

variations in hydrogen bonds as a function of pressure exert a crucial function in the structural stability of materials.

Biurea ($C_2H_6N_4O_2$) has attracted considerable research interest because of its structural and characteristic properties at ambient and high-temperature conditions. The compound has a wide range of applications and unique properties. For example, biurea is primarily used in industry as a high-temperature blowing agent for expanding plastics such as polypropylene. It is also a major product of the thermal decomposition of azodicarbonamide, which is a new flour gluten fortifier. Biurea reportedly decomposes in the temperature range of 230−260 °C to yield gas, a white sublimate, and a viscous liquid residue.[43] In terms of structure, biurea can be regarded as two urea molecules connected via the removal of two H atoms. In view of its simple structure, biurea is a model system for studying the structure and phase stability of hydrogen-bonded molecular crystals under high pressures. The crystal and molecular structure of biurea at ambient conditions were determined by Brown and Russell in 1976.[44] The compound crystallizes into a monoclinic structure with the $C2/c$ space group, the unit cell parameters of which are a = 15.78(0) Å, b = 4.63(7) Å, c = 9.33(1) Å, β = 133.84(0)°, V = 492.46(4) Å^3, and Z = 4. As shown in Figure 1, the molecule as a whole is nonplanar because the two symmetry-related halves of the molecule are inclined at 83.6° relative to each another. Biurea also exhibits ordinary three-dimensional hydrogen-bonded networks where molecules are held together by extensive hydrogen bonds. Each of the six hydrogen atoms of the compound is hydrogen-bonded to an oxygen atom in the neighboring molecule. Each O atom is involved in close contact with three separate NH groups. The molecule therefore presents in a total of six donors and six acceptors, forming 12 N−H···O hydrogen bonds.

In the present work, we report the Raman scattering and angle-dispersive X-ray diffraction (ADXRD) patterns of biurea obtained in a diamond anvil cell (DAC) at room temperature and pressures of up to ∼5 GPa. Reversible phase transition from $C2/c$ to $P2/n$ was confirmed. Both external (intermolecular) and internal (intramolecular) modes were detected and analyzed in the Raman experiments to provide detailed information on the motions of molecular fragments and hydrogen bonds. Data of structural conformations in the high-pressure phase were obtained from the ADXRD patterns. Analysis of structural changes and cooperative effects between hydrogen bonding and van der Waals interactions was also performed. The present study provides an improved understanding of the behavior of hydrogen-bonded networks and explores the effects of intermolecular interactions on the stability of hydrogen-bonded molecular crystals.

EXPERIMENTAL SECTION

Biurea was purchased from Alfa Aesar and used as received. A symmetric DAC with 400 μm culet-size diamonds was used for *in situ* high-pressure measurements. A T301 stainless steel gasket was preindented to a thickness of 50 μm, and a center hole drilled to a diameter of 130 μm was used as the sample chamber. The powder sample was loaded into the hole together with one or two small ruby chips. A 4:1 (v/v) mixture of methanol and ethanol was used as the pressure-transmitting medium (PTM).[45] Meanwhile, the high-pressure Raman scattering experiment with liquid nitrogen as the PTM was conducted. Nitrogen, at ambient temperature, freezes into a plastic crystal that is very soft. Methanol−ethanol mixtures are highly viscous and become more rigid with pressure. Therefore, the liquid nitrogen will provide better hydrostatic conditions than the methanol−ethanol mixtures below 5 GPa. However, the results under the two pressure media are essentially the same, implying that the structural phase transition is not affected by the ethanol or methanol, which has strong hydrogen bonding (Figures S1, Supporting Information). The pressure was determined using the well-established ruby fluorescence technique with an uncertainty of ±0.05 GPa under hydrostatic conditions. All of the experiments were conducted at room temperature.

Raman measurements were carried out using an Acton SpectraPro 2500i spectrometer. The 532 nm line of a diode laser was applied as the excitation source. The laser output power on the sample was kept to 10 mW. Raman scattering was determined using a backscattering configuration. Raman signals were recorded using a liquid nitrogen cooled CCD camera (Pylon, 100B) with the spectral resolution set to 1 cm^{-1}. Raman profiles were fit when necessary using a combination of Gaussian and Lorentzian functions.

ADXRD experiments were conducted on the BL15U1 beamline at the Shanghai Synchrotron Radiation Facility (SSRF). Part of the synchrotron XRD measurements were conducted at the 4W2 beamline at the High Pressure Station of the Beijing Synchrotron Radiation Facility (BSRF). All experiments were performed at room temperature. A monochromatic 0.6199 Å beam was utilized for pattern collection. Prior to each experiment, CeO_2 was used as a standard sample for calibration of geometric parameters. Typical Bragg diffraction rings were recorded with a Mar345

dx.doi.org/10.1021/jp503803n | J. Phys. Chem. C 2014, 118, 15162−15168

imaging-plate detector. The 2-D images collected were integrated and converted into plots of intensity versus 2θ using the Fit2D program. ADXRD patterns were then indexed and refined by the Rietveld method using the reflex module included in the Materials Studio 5.5 program (Accelrys Inc.).

RESULTS AND DISCUSSION

The point group symmetry of the biurea molecule is $C_{2h}(2/m)$. The mechanical representation of this symmetry is

$$M = 21A_g + 21A_u + 21B_g + 21B_u$$

showing 3 acoustic modes

$$\Gamma_{acoustic} = A_u + 2B_u$$

and 81 optic modes

$$\Gamma_{optic} = 21A_g + 20A_u + 21B_g + 19B_u$$

Group-theoretical analysis of the vibrations shows that, among the 81 optical modes, the Raman-active modes belong to $21A_g + 21B_g$ symmetry and the infrared-active modes belong to $20A_u + 19B_u$ symmetry. Some of the Raman modes could not be observed in our experiments because of the very weak intensities and limited splitting between correlation components. Assignments for the Raman modes of biurea are based on the literature.[46−48]

Figure 2 shows the Raman spectra of the external modes; here translational and librational vibrations at several pressures

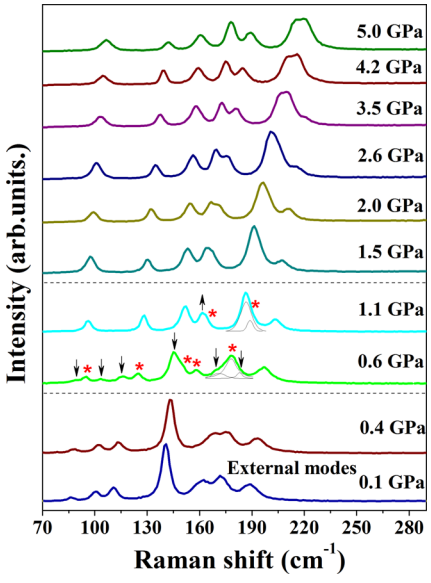

Figure 2. Evolution of external modes in biurea at various pressures in the range of 70−290 cm^{-1}. The asterisks denote the emergence of new peaks, and the down arrows show the disappearance of the peaks.

are observed. The corresponding peak positions versus pressure are depicted in Figure 3. The spectrum at 0.1 GPa consists of seven external modes (86, 99, 110, 140, 162, 172, and 188 cm^{-1}). At 0.6 GPa, new external modes emerge, as marked by asterisks, which indicate the beginning of phase transition from phase I to high-pressure phase II. Another two external modes, again marked with an asterisk, are observed at 1.1 GPa; the appearance of these modes is accompanied by the disappearance of modes marked with downward-facing arrows. The relative intensity of the mode with an upward-facing arrow

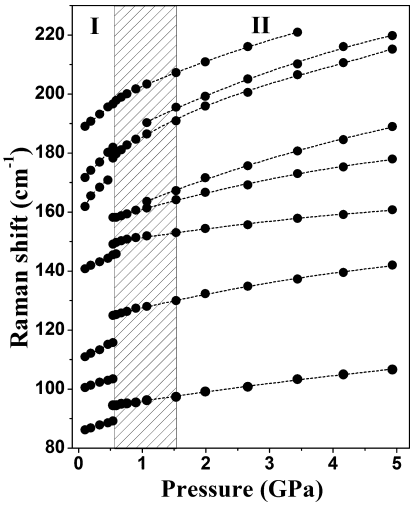

Figure 3. Pressure dependence of Raman peak positions of the corresponding external modes. The shadow region represents the boundary of ambient phase I and high-pressure phase II.

continues to increase. As the pressure is raised to 0.1 GPa, the band at 188 cm^{-1} gradually loses its intensity; at 4.2 GPa, this band completely disappears into the scattering background eventually at 4.2 GPa. Upon further compression to 5 GPa, the new pattern of peaks remains essentially similar to that at 1.5 GPa, implying that phase II is stable and does not undergo further changes up to the highest pressure employed in this experiment. As shown in Figure 3, significant discontinuities occur over the pressure range of 0.6−1.5 GPa, consistent with the proposed phase transition. Beyond the phase transition, all Raman bands in the external region exhibit normal blue shifts. These blue shifts indicate external modes hardening because of the enhancements in intermolecular interactions.[49,50]

The evolution of the Raman spectra in the range of 410−1800 cm^{-1} as a function of pressure is summarized in Figure 4. The internal modes are related to the vibrations of a specific group and can be used to explore local variations in the chemical environment around specific groups. For these internal modes, considerable variations in the spectrum can be detected. The C═O in-plane bending (584 and 604 cm^{-1}), O═C−N in-plane bending (986 and 1004 cm^{-1}), and NH_2 scissoring modes (1603 and 1619 cm^{-1}) evolve into triplet bands at 0.6 GPa. Similarly, the N−N out-of-plane bending mode (1241 cm^{-1}) shows asymmetry and marked 2-fold splitting at this pressure, as shown in Figure 4b. A new peak emerges at 1083 cm^{-1} around the NH_2 out-of-plane bending mode. Splitting of the existing modes and the appearance of new modes reveal the lowering of crystalline symmetry as well as changes in the local chemical environment around C, N, and O atoms due to phase transition. When the pressure reaches 1.1 GPa, a new mode appears at 620 cm^{-1} with gradually increasing high intensity. Modes marked with downward-facing arrows completely lose their intensities, whereas the three modes marked with upward-facing arrows show continuous increases in intensity. These considerable variations imply that the proposed phase transition of biurea involves a large conformational change in the molecule. The pressure dependence of peak positions of the corresponding internal modes is depicted in Figure 5. All of the internal modes exhibit changes in slope across the transition pressure and shift gradually toward higher frequencies, as a result of the decrease in interatomic distances

dx.doi.org/10.1021/jp503803n | J. Phys. Chem. C 2014, 118, 15162−15168

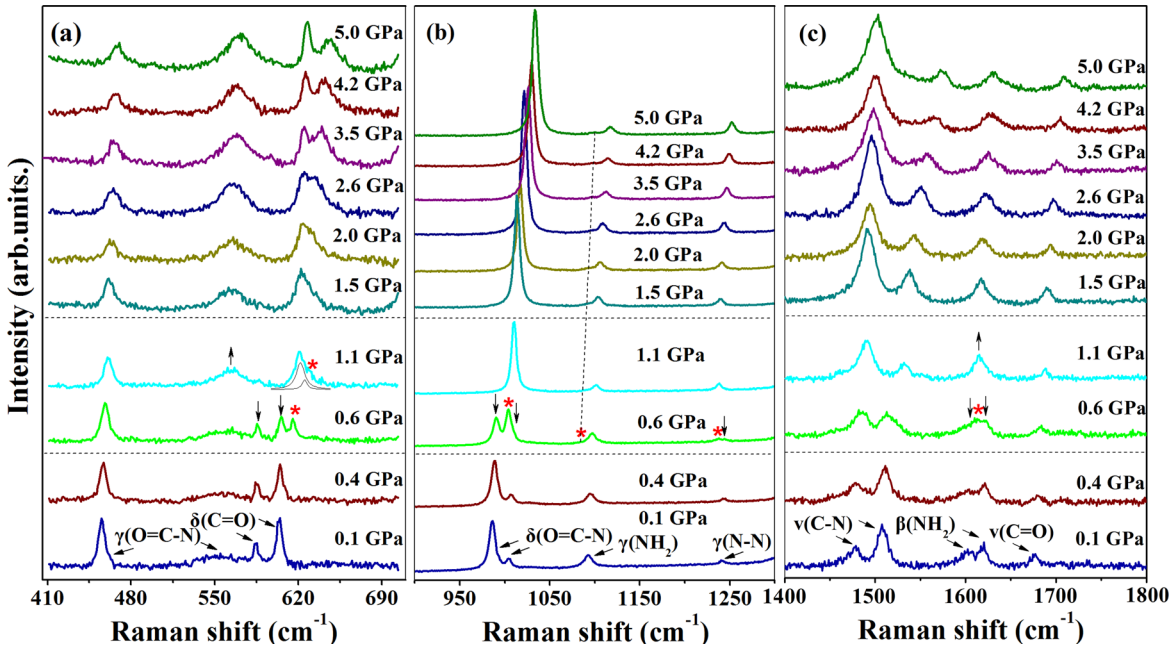

Figure 4. Selected Raman spectra of biurea at various pressures in the ranges of (a) 410−700, (b) 900−1300, and (c) 1400−1800 cm^{-1}.

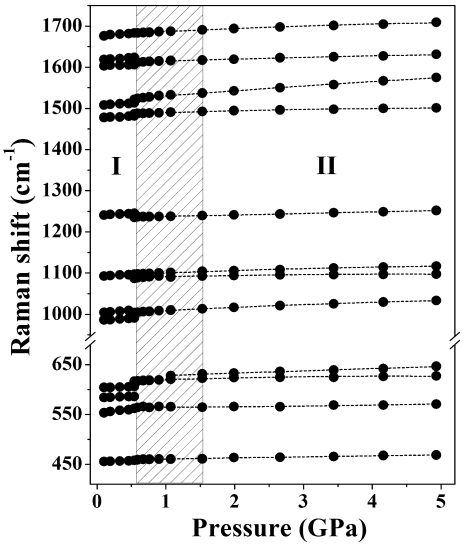

Figure 5. Frequency shifts of the selected internal modes in the range of 410−1800 cm^{-1} as a function of pressure. Linear fits are performed for clarity. The shadow region represents the boundary of phase I and phase II.

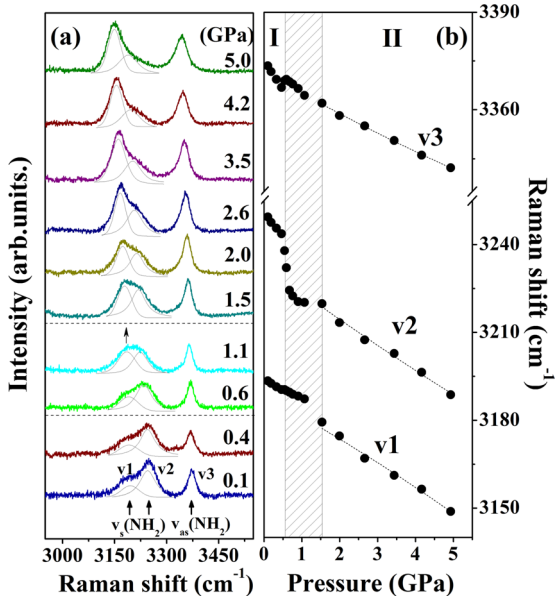

Figure 6. Raman spectra of biurea at different pressures in the NH_2 stretching region of 2950−3550 cm^{-1} (a); frequency shifts of these modes (b). The shadow region represents the boundary of the two phases.

and increase in effective force constants.[51,52] These internal modes exhibit much smaller shift rates compared with external modes because covalent bonds are stronger and show much lower compressibility than noncovalent bonds.

In Figure 6, we present Raman spectra in the NH_2 stretching region and frequency shifts at selected pressures. At 0.1 GPa, three modes can be detected (labeled ν_1 to ν_3). Mode ν_1 at 3180 cm^{-1} and mode ν_2 at 3250 cm^{-1} are identified as symmetric stretching vibrations; mode ν_3 at 3400 cm^{-1} corresponds to asymmetric stretching vibrations. The two symmetric stretching modes undergo complete reversal of intensity, and mode ν_2 gradually merges with mode ν_1. Below 0.6 GPa, mode ν_1 has a higher intensity than mode ν_2. However, mode ν_2 progressively gains intensity with increasing pressure. As the pressure is increased up to 1.5 GPa, mode ν_1 shows reductions in intensity relative to mode ν_2, which indicates accomplishment of phase transition. Detailed information on the peak positions versus pressure is shown in Figure 6b. Overall, the three NH_2 stretching modes show red shifts, although these shifts occur at different rates. The red shifts suggest the presence of weak or moderate strength N−H···O hydrogen bonds in biurea crystals.[53−56] For weak and moderate hydrogen bonds, pressure can shorten the H···O distance, resulting in increased electrostatic attraction between H and O. The N−H distance is then extended, causing red shifts of the NH_2 stretching modes. The red shifts observed agree well with the blue shift of NH_2 out-of-plane bending vibrations (1095 cm^{-1}). The

dx.doi.org/10.1021/jp503803n | J. Phys. Chem. C 2014, 118, 15162−15168

discontinuities of frequency shifts in the pressure range of 0.6−1.5 GPa confirm that the proposed phase transition is related to changes in the N−H···O hydrogen-bonded sheets.

To confirm the phase transition of biurea and understand the structural variations that occur under high-pressure conditions, we conducted an ADXRD experiment. Representative ADXRD patterns of biurea at various pressures are shown in Figure 7. At

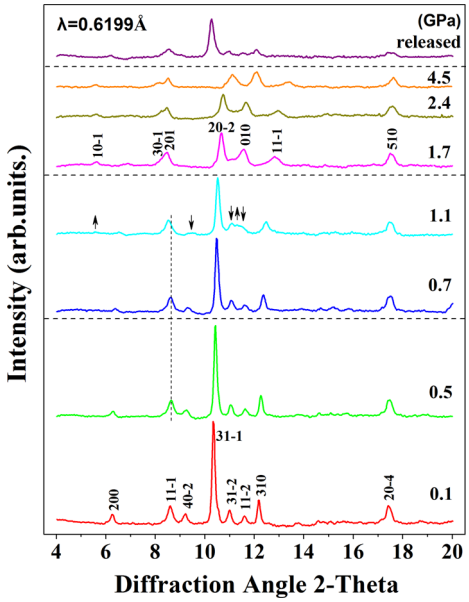

Figure 7. Representative ADXRD patterns of biurea at high pressures with the 4:1 methanol−ethanol mixture as PTM. The wavelength for data collection is 0.6199 Å.

0.7 GPa, the $(11\bar{1})$ peak shifts to a lower angle which continues to decrease over the pressure range of 0.7−1.1 GPa. At 1.1 GPa, two new peaks, marked with upward-facing arrows, emerge and gradually gain intensity. The $(40\bar{2})$, $(31\bar{2})$, and $(11\bar{2})$ peaks vanish completely when the pressure reaches 1.7 GPa. These changes provide sufficient evidence of the phase transition of biurea. Above 1.7 GPa, the $(30\bar{1})$ peak shifts to lower angle, which is attributed to the increase in interplanar distance caused by molecular rotation. Besides this peak, all other diffraction peaks shift to higher angles with increasing pressure as a result of the decrease in *d*-spacings. Figure 8 shows the Rietveld refinement result of the ADXRD pattern at 1.7 GPa. The inset in Figure 8 illustrates the refined crystal structure of phase II. Phase II might be indexed to a monoclinic symmetry with a possible space group *P*2/*n*. The indexed lattice constants obtained were a = 14.52(0) Å, b = 3.06(4) Å, c = 6.66(3) Å, and β = 108.61(5)°, and the unit cell volume V = 280.96(9) Å^3 with Z = 4. No significant variation of the diffraction patterns of phase II is observed, which indicates that the high-pressure phase is stable up to the highest pressure employed in our experiment. Upon release of pressure, the diffraction pattern of phase II returns to its initial state; this finding reveals that the phase transition observed is reversible.

The Raman and ADXRD results provide strong evidence of the pressure-induced phase transition of biurea. A mechanism for the phase transition is proposed based on the experimental results. A comparison of the structures of the two phases is illustrated in Figure 9. Hydrogen bonding and van der Waals interactions have proven to be dominant interactions for the crystal packing of biurea at ambient pressure. Below 0.6 GPa,

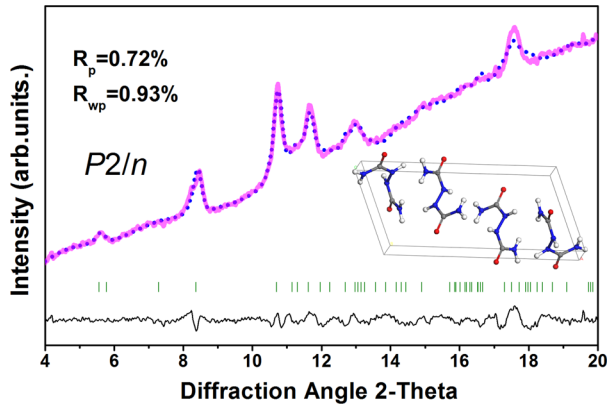

Figure 8. Rietveld refinement of the ADXRD pattern at ∼1.7 GPa: pink line, experimental; blue dotted line, simulated; black line, residual pattern. The inset shows the possible crystal structure of high-pressure phase II.

modes related to N−H···O hydrogen bonds, including C═O in-plane bending, O═C−N in-plane bending, NH_2 out-of-plane bending, and NH_2 scissoring, exhibit blue shifts without abrupt changes. Increases in pressure induce adjacent molecules to come into closer contact with each other, thereby strengthening hydrogen bonding and van der Waals interactions. Upon further compression in the range of 0.6−1.5 GPa, biurea no longer supports intermolecular interactions and rearrangement of the hydrogen-bonded networks occur to reduce the intermolecular interactions; these changes result in symmetry transformation from *C*2/*c* to a possible space group *P*2/*n*. The proposed mechanism can be well-supported by the Raman results. The external modes involve the collective motions of all atoms in the unit cell and exert an important function in monitoring structural changes under high pressures. Drastic changes in these external modes, such as the disappearance of numerous peaks and appearance of new peaks, suggest that great changes in intermolecular interactions take place. Various variations of the Raman modes related to N−H···O hydrogen bonds also confirm the rearrangement of hydrogen-bonded networks in biurea during phase transition. As can be seen from the spectra obtained, the C═O in-plane bending and O═C−N in-plane bending modes evolve into triplet bands, which indicates twisting of the C═O bonds. Thus, acceptors of the hydrogen bonds adopt new orientations. As well, the NH_2 out-of-plane bending and NH_2 scissoring modes, which provide N atoms as hydrogen bond donors, show asymmetry and splitting; thus, N−H bonds also undergo rotation. Overall, rearrangement of the hydrogen-bonded networks causes molecular rotation and translation, ultimately resulting in phase transition. Meanwhile, rotations of the molecular functional groups and complicated distortions of hydrogen bonds in biurea lead to the relatively large pressure range of the phase transition. After releasing pressure, these deformed molecules and distorted hydrogen bonds are recovered, so the high-pressure structure returns to the ambient state. High-pressure neutron diffraction studies are necessary to provide reliable information on the hydrogen atomic positions.

CONCLUSION

In summary, we performed high-pressure studies of biurea using Raman spectroscopy and angle-dispersive X-ray diffraction (ADXRD). Both Raman and ADXRD data provide sufficient evidence of the phase transition of the compound

dx.doi.org/10.1021/jp503803n | J. Phys. Chem. C 2014, 118, 15162−15168

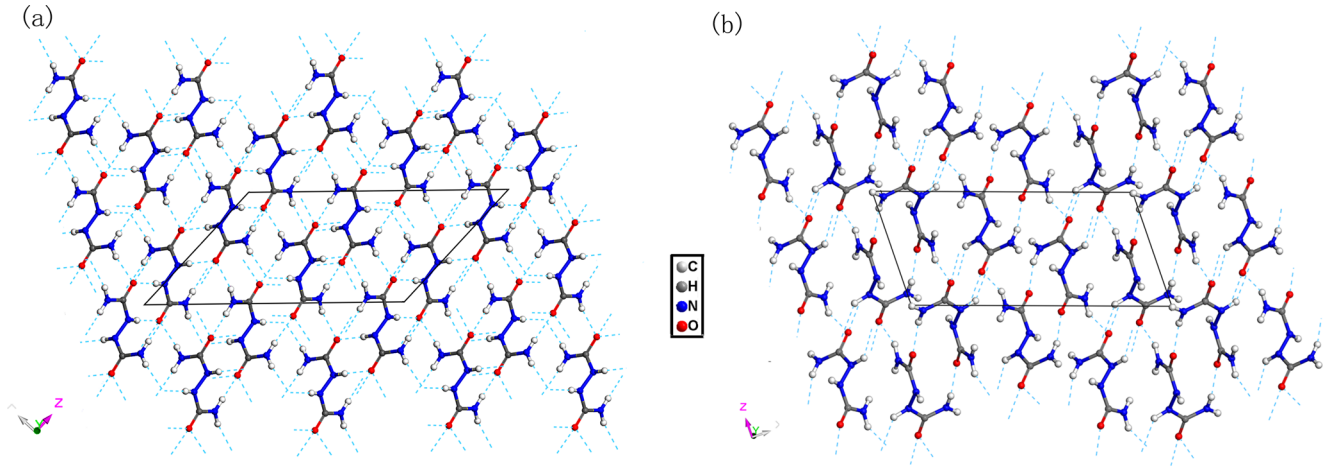

Figure 9. Crystal structures and hydrogen-bonded networks of biurea: (a) ambient phase I; (b) possible high-pressure phase II. Hydrogen bonds N−H···O are marked as dashed lines.

in the pressure range of 0.6−1.5 GPa; the high-pressure phase is stable up to ∼5 GPa. The X-ray diffraction data are consistent with a high-pressure structure change from $C2/c$ to the proposed space group $P2/n$. Variations in the Raman modes related to N−H···O hydrogen bonds indicate that the mechanism of phase transition involves rearrangement of the hydrogen-bonded networks, according to the various variations of the Raman modes related to N−H···O hydrogen bonds. The present study helps improve the current understanding on the nature of hydrogen bonds as well as cooperative effects of various noncovalent interactions under high-pressure conditions.

■ ASSOCIATED CONTENT

Supporting Information

Selected high-pressure Raman spectra of biurea under different kinds of pressure conditions (one with the methanol−ethanol mixtures as the pressure-transmitting medium (PTM) and one with liquid nitrogen as the PTM (Figure S1)) and C, N, and O atom positions of the proposed high-pressure phase II of biurea from Rietveld refinement (Table S1). This material is available free of charge via the Internet at http://pubs.acs.org.

■ AUTHOR INFORMATION

Corresponding Authors

*(B.Z.) E-mail: zoubo@jlu.edu.cn. Tel.: +86-0431-85168882.
*(K.W.) E-mail: kaiwang@jlu.edu.cn. Tel.: +86-0431-85168882.

Notes

The authors declare no competing financial interest.

■ ACKNOWLEDGMENTS

This work is supported by NSFC (Grant Nos. 91227202 and 11204101), RFDP (Grant No. 20120061130006), National Basic Research Program of China (Grant No. 2011CB808200), China Postdoctoral Science Foundation (Grant No. 2012M511327), and Project 2014087 Supported by the Graduate Innovation Fund of Jilin University. ADXRD measurement was performed at the 15U1 beamline of the Shanghai Synchrotron Radiation Facility (SSRF). Portions of this work were performed at the 4W2 beamline, Beijing Synchrotron Radiation Facility (BSRF) that is supported by the Chinese Academy of Sciences (Grant Nos. KJCX2-SW-N03 and KJCX2-SW-N20).

■ REFERENCES

(1) Steiner, T. The Hydrogen Bond in the Solid State. *Angew. Chem., Int. Ed.* **2002**, *41*, 48−76.
(2) Aakeröy, C. B.; Seddon, K. R. The Hydrogen Bond and Crystal Engineering. *Chem. Soc. Rev.* **1993**, *22*, 397−407.
(3) Dunitz, J. D.; Gavezzotti, A. Molecular Recognition in Organic Crystals: Directed Intermolecular Bonds or Nonlocalized Bonding? *Angew. Chem., Int. Ed.* **2005**, *44*, 1766−1787.
(4) Fillaux, F. Hydrogen Bonding and Quantum Dynamics in the Solid State. *Int. Rev. Phys. Chem.* **2000**, *19*, 553−564.
(5) Desiraju, G. R. Hydrogen Bridges in Crystal Engineering: Interactions without Borders. *Acc. Chem. Res.* **2002**, *35*, 565−573.
(6) Luzar, A.; Chandler, D. Hydrogen-Bond Kinetics in Liquid Water. *Nature* **1996**, *379*, 55−57.
(7) Wang, K.; Duan, D. F.; Wang, R.; Liu, D.; Tang, L.; Cui, T.; Liu, B. B.; Cui, Q.; Liu, J.; Zou, B. Pressure-Induced Phase Transition in Hydrogen-Bonded Supramolecular Adduct Formed by Cyanuric Acid and Melamine. *J. Phys. Chem. B* **2009**, *113*, 14719−14724.
(8) Minkov, V. S.; Krylov, A. S.; Boldyreva, E. V.; Goryainov, S. V.; Bizyaev, S. N.; Vtyurin, A. N. Pressure-Induced Phase Transitions in Crystalline L-and DL-Cysteine. *J. Phys. Chem. B* **2008**, *112*, 8851−8854.
(9) Mishra, A. K.; Murli, C.; Sharma, S. M. High Pressure Raman Spectroscopic Study of Deuterated γ-Glycine. *J. Phys. Chem. B* **2008**, *112*, 15867−15874.
(10) Goryainov, S.; Boldyreva, E.; Kolesnik, E. Raman Observation of a New (ζ) Polymorph of Glycine? *Chem. Phys. Lett.* **2006**, *419*, 496−500.
(11) Goncharov, A. F.; Struzhkin, V. V.; Mao, H.-k.; Hemley, R. J. Raman Spectroscopy of Dense H_2O and the Transition to Symmetric Hydrogen Bonds. *Phys. Rev. Lett.* **1999**, *83*, 1998.
(12) Bernasconi, M.; Silvestrelli, P.; Parrinello, M. Ab Initio Infrared Absorption Study of the Hydrogen-Bond Symmetrization in Ice. *Phys. Rev. Lett.* **1998**, *81*, No. 1235.
(13) Goncharov, A. F.; Manaa, M. R.; Zaug, J. M.; Gee, R. H.; Fried, L. E.; Montgomery, W. B. Polymerization of Formic Acid under High Pressure. *Phys. Rev. Lett.* **2005**, *94*, No. 065505.
(14) Yan, T. T.; Wang, K.; Tan, X.; Liu, B. B.; Zou, B. *p*-Aminobenzoic Acid Polymorphs under High Pressures. *RSC Adv.* **2014**, *4*, 15534−15541.
(15) Mookherjee, M.; Stixrude, L. High-Pressure Proton Disorder in Brucite. *Am. Mineral.* **2006**, *91*, 127−134.
(16) Kuo, J.-L.; Klein, M. L.; Kuhs, W. F. The Effect of Oroton Disorder on theStructure of Ice-Ih: A Theoretical Study. *J. Chem. Phys.* **2005**, *123*, No. 134505.

(17) Yan, T. T.; Li, S. R.; Wang, K.; Tan, X.; Jiang, Z. M.; Yang, K.; Liu, B. B.; Zou, G. T.; Zou, B. Pressure-Induced Phase Transition in N−H···O Hydrogen-Bonded Molecular Crystal Oxamide. *J. Phys. Chem. B* **2012**, *116*, 9796−9802.
(18) Wang, K.; Duan, D. F.; Wang, R.; Lin, A.; Cui, Q.; Liu, B. B.; Cui, T.; Zou, B.; Zhang, X.; Hu, J. Z.; et al. Stability of Hydrogen-Bonded Supramolecular Architecture under High Pressure Conditions: Pressure-Induced Amorphization in Melamine− Boric Acid Adduct. *Langmuir* **2009**, *25*, 4787−4791.
(19) Tan, X.; Wang, K.; Li, S. R.; Yuan, H. S.; Yan, T. T.; Liu, J.; Yang, K.; Liu, B. B.; Zou, G. T.; Zou, B. Exploration of the Pyrazinamide Polymorphism at High Pressure. *J. Phys. Chem. B* **2012**, *116*, 14441−14450.
(20) Wang, K.; Liu, J.; Yang, K.; Liu, B. B.; Zou, B. High-Pressure-Induced Polymorphic Transformation of Maleic Hydrazide. *J. Phys. Chem. C* **2014**, *118*, 8122−8127.
(21) Bastea, M.; Bastea, S.; Reaugh, J. E.; Reisman, D. B. Freezing Kinetics in Overcompressed Water. *Phys. Rev. B* **2007**, *75*, No. 172104.
(22) Fanetti, S.; Lapini, A.; Pagliai, M.; Citroni, M.; Di Donato, M.; Scandolo, S.; Righini, R.; Bini, R. Structure and Dynamics of Low-Density and High-Density Liquid Water at High Pressure. *J. Phys. Chem. Lett.* **2013**, *5*, 235−240.
(23) Schwegler, E.; Galli, G.; Gygi, F. Water under Pressure. *Phys. Rev. Lett.* **2000**, *84*, No. 2429.
(24) Sun, C. Q.; Zhang, X.; Zheng, W. The Hidden Force Opposing Ice Compression. *Chem. Sci.* **2012**, *3*, 1455−1460.
(25) Chen, J.-Y.; Yoo, C.-S. High Density Amorphous Ice at Room Temperature. *Proc. Natl. Acad. Sci. U. S. A.* **2011**, *108*, 7685−7688.
(26) Wang, Y.; Liu, H.; Lv, J.; Zhu, L.; Wang, H.; Ma, Y. High Pressure Partially Ionic Phase of Water Ice. *Nat. Commun.* **2011**, *2*, 563.
(27) Dawson, A.; Allan, D. R.; Belmonte, S. A.; Clark, S. J.; David, W. I.; McGregor, P. A.; Parsons, S.; Pulham, C. R.; Sawyer, L. Effect of High Pressure on the Crystal Structures of Polymorphs of Glycine. *Cryst. Growth Des.* **2005**, *5*, 1415−1427.
(28) Boldyreva, E.; Sowa, H.; Seryotkin, Y. V.; Drebushchak, T.; Ahsbahs, H.; Chernyshev, V.; Dmitriev, V. Pressure-Induced Phase Transitions in Crystalline L-Serine Studied by Single-Crystal and High-Resolution Powder X-ray Diffraction. *Chem. Phys. Lett.* **2006**, *429*, 474−478.
(29) Staun Olsen, J.; Gerward, L.; Souza Filho, A.; Freire, P.; Mendes Filho, J.; Melo, F. High-Pressure X-ray Diffraction of L-ALANINE Crystal. *High Pressure Res.* **2006**, *26*, 433−437.
(30) Wang, R.; Li, S. R.; Wang, K.; Duan, D. F.; Tang, L.; Cui, T.; Liu, B. B.; Cui, Q. L.; Liu, J.; Zou, B. Pressure-Induced Phase Transition in Hydrogen-Bonded Supramolecular Structure: Guanidinium Nitrate. *J. Phys. Chem. B* **2010**, *114*, 6765−6769.
(31) Olejniczak, A.; Ostrowska, K.; Katrusiak, A. H-Bond Breaking in High-Pressure Urea. *J. Phys. Chem. C* **2009**, *113*, 15761−15767.
(32) Hermet, P.; Ghosez, P. First-Principles Study of the Dynamical and Nonlinear Optical Properties of Urea Single Crystals. *Phys. Chem. Chem. Phys.* **2010**, *12*, 835−843.
(33) Andersson, O.; Ross, R. Phase Behavior and Thermal Conductivity of Urea at Pressures up to 1 GPa and at Temperatures in the Range 50−370 K. *Int. J. Thermophys.* **1994**, *15*, 513−524.
(34) Yang, G.; Li, Y.; Dreger, Z.; White, J.; Drickamer, H. High-Pressure Studies of Second Harmonic Generation in Organic Materials. *Chem. Phys. Lett.* **1997**, *280*, 375−380.
(35) Bridgman, P. W. Polymorphic Transitions up to 50,000 kg/Cm^2 of Several Organic Substances. *Proc. Am. Acad. Arts Sci.* **1938**, *72*, 227−268.
(36) Marshall, W. G.; Francis, D. J. Attainment of Near-Hydrostatic Compression Conditions Using the Paris-Edinburgh Cell. *J. Appl. Crystallogr.* **2002**, *35*, 122−125.
(37) Bonin, M.; Marshall, W. G.; Weber, H.-P.; Toledano, F. *ISIS Pulsed Neutron and Muon Source*, Annual Report 1998; Rutherford Appleton Laboratory: Didcot, U.K., 1998; pp 34−35.
(38) Hamann, S. D.; Linton, M. The Influence of Pressure on the Infrared Spectra of Hydrogen-Bonded Solids. I. Compounds with OH···O Bonds. *Aust. J. Chem.* **1975**, *28*, 2567−2578.
(39) Lamelas, F.; Dreger, Z.; Gupta, Y. Raman and X-ray Scattering Studies of High-Pressure Phases of Urea. *J. Phys. Chem. B* **2005**, *109*, 8206−8215.
(40) Figuiere, P.; Ghelfenstein, M.; Szwarc, H. First-Order Phase Diagram of Thiourea and Raman Spectroscopy. *Chem. Phys. Lett.* **1975**, *33*, 99−103.
(41) Banerji, A.; Deb, S. Raman Scattering Study of High-Pressure Phase Transition in Thiourea. *J. Phys. Chem. B* **2007**, *111*, 10915−10919.
(42) Asahi, T.; Hasebe, K.; Onodera, A. Crystal Structure of the High Pressure Phase VI of Thiourea. *J. Phys. Soc. Jpn.* **2000**, *69*, 2895−2899.
(43) Russell, P. R.; Strachan, A. N. The Thermal Decomposition of Biurea. *J. Chem. Soc., Perkin Trans. 2* **1978**, 323−326.
(44) Brown, D.; Russell, P. The Crystal and Molecular Structure of Biurea. *Acta Crystallogr.* **1976**, *32*, 1056−1058.
(45) Audrieth, D. C.; Mohr, E. B. Biurea. *Inorg. Synth.* **1953**, *4*, 26−28.
(46) Xie, Y.; Li, P.; Zhang, J.; Wang, H.; Qian, H.; Yao, W. Comparative Studies by IR, Raman, and Surface-Enhanced Raman Spectroscopy of Azodicarbonamide, Biurea and Semicarbazide Hydrochloride. *Spectrochim. Acta* **2013**, *114*, 80−84.
(47) Kraebel, C. M.; Davis, S. M.; Landon, M. J. Hydrazine Derivatives—I. Infrared Spectra of Biureas, 1,1′-Azobisformamides and Hydrazine Disulfonic Acid Derivatives. *Spectrochim. Acta* **1967**, *23*, 2541−2549.
(48) Mashima, M. The Infrared Absorption Spectra of $(NH_2CONH-)_2$, $NH_2CONHNH_2$, $(NH_2CSNH-)_2$ and $NH_2CSNHNH_2$. *Bull. Chem. Soc. Jpn.* **1964**, *37*, 974−984.
(49) Park, T.-R.; Dreger, Z. A.; Gupta, Y. M. Raman Spectroscopy of Pentaerythritol Single Crystals under High Pressures. *J. Phys. Chem. B* **2004**, *108*, 3174−3184.
(50) Ciezak, J. A.; Jenkins, T. A.; Liu, Z.; Hemley, R. J. High-Pressure Vibrational Spectroscopy of Energetic Materials: Hexahydro-1,3,5-trinitro-1,3,5-triazine. *J. Phys. Chem. A* **2007**, *111*, 59−63.
(51) Rao, R.; Sakuntala, T.; Godwal, B. Evidence for High-Pressure Polymorphism in Resorcinol. *Phys. Rev. B* **2002**, *65*, No. 054108.
(52) Franco, O.; Orgzall, I.; Regenstein, W.; Schulz, B. Structural and Spectroscopical Study of a 2,5-Diphenyl-1, 3, 4-oxadiazole Polymorph under Compression. *J. Phys.: Condens. Matter* **2006**, *18*, No. 1459.
(53) Hamann, S. D.; Linton, M. The Influence of Pressure on the Infrared Spectra of Hydrogen-Bonded Solids. III. Compounds with NH···X Bonds. *Aust. J. Chem.* **1976**, *29*, 1641−1647.
(54) Reynolds, J.; Sternstein, S. S. Effect of Pressure on the Infrared Spectra of Some Hydrogen-Bonded Solids. *J. Chem. Phys.* **2004**, *41*, 47−50.
(55) Pravica, M.; Yulga, B.; Liu, Z.; Tschauner, O. Infrared Study of 1,3,5-triamino-2,4,6-Trinitrobenzene under High Pressure. *Phys. Rev. B* **2007**, *76*, No. 064102.
(56) Moon, S.; Drickamer, H. Effect of Pressure on Hydrogen Bonds on Organic Solids. *J. Chem. Phys.* **2003**, *61*, 48−54.